

Nuclear structure of the spin-isospin excited states in ^{13}N studied via the $(^3\text{He},t)$ and $(^3\text{He},tp)$ reactions at 450 MeV

H. Fujimura,¹ H. Akimune,² I. Daito,³ M. Fujiwara,^{1,4} K. Hara,¹ K. Y. Hara,² M. N. Harakeh,⁵ F. Ihara,¹ T. Inomata,¹ K. Ishibashi,¹ T. Ishikawa,⁶ T. Kawabata,⁷ A. Tamii,⁸ M. Tanaka,⁹ H. Toyokawa,¹⁰ T. Yamanaka,¹ and M. Yosoi⁶

¹Research Center for Nuclear Physics, Osaka University, Ibaraki, Osaka 567-0047, Japan

²Department of Physics, Konan University, Kobe, Hyogo 658-8501, Japan

³Advanced Photon Research Center, Japan Atomic Energy Research Institute, Kizu, Kyoto 619-0215, Japan

⁴Advanced Science Research Center, Japan Atomic Energy Research Institute, Tokai, Ibaraki 319-1195, Japan

⁵Kernfysisch Versneller Instituut, NL-9747 AA Groningen, The Netherlands

⁶Department of Physics, Kyoto University, Kyoto 606-8502, Japan

⁷Center for Nuclear Study, Graduate School of Science, University of Tokyo, Bunkyo, Tokyo 113-0033, Japan

⁸Department of Physics, University of Tokyo, Hongo, Tokyo 113-0033, Japan

⁹Kobe Tokiwa Junior College, Nagataku, Kobe 653-0838, Japan

¹⁰Japan Synchrotron Radiation Research Institute, Hyogo 679-5198, Japan

(Received 12 February 2004; published 30 June 2004)

Spin-isospin excitations in ^{13}N have been studied by means of the $(^3\text{He},t)$ and $(^3\text{He},tp)$ reactions at a bombarding energy of $E(^3\text{He})=450$ MeV. The zero-degree $(^3\text{He},t)$ spectrum is found to be similar to those from the (p,n) reactions at intermediate energies, suggesting a simple direct reaction mechanism at $E(^3\text{He})=450$ MeV. The Gamow-Teller (GT) states with $J^\pi=1/2^-$ and $3/2^-$ have been strongly excited at $\theta_{\text{lab}}=0^\circ$. The angular distribution of cross sections for the $^{13}\text{C}(^3\text{He},t)^{13}\text{N}$ reaction and the elastic ^3He scattering off ^{13}C were obtained at $\theta_{\text{lab}}=0^\circ-17^\circ$ and at $\theta_{\text{lab}}=2^\circ-22^\circ$, respectively. The obtained experimental results were compared with calculations performed in distorted-wave Born approximation. Microscopic structures of the states in ^{13}N have further been studied by observing decay protons in coincidence with high-energy tritons measured at $\theta_{\text{lab}}=0^\circ$. The branching ratios for proton decay from the GT states in ^{13}N to the final low-lying $T=0$ states in ^{12}C were obtained. The wave functions of the excited states in ^{13}N are discussed on the basis of obtained experimental data and relevant theoretical calculations.

DOI: 10.1103/PhysRevC.69.064327

PACS number(s): 24.30.Cz, 25.55.Kr, 29.30.Ep, 27.20.+n

I. INTRODUCTION

The study of the nuclear structure of the $A=13$ mirror nuclei is an interesting subject from the point of view of isospin symmetry. The levels in ^{13}C and ^{13}N are isobaric mirrors. The isobaric relation between ^{13}C and ^{13}N is basically valid although small isospin violation is caused by differences in the radial wave functions due to differences in the binding energies. These small effects are actually observed in the mirror γ decays from the lowest $T=3/2$ level in ^{13}C and ^{13}N . The Seattle group [1] reported that the $E1$ γ decay from the $T=3/2$, 15 MeV analog states in ^{13}C and ^{13}N shows a pronounced charge asymmetry, which is not explained by simple binding-energy effects.

In the past, protons emitted from the $T=3/2$, $3/2^-$ state at $E_x=15.06$ MeV in ^{13}N were measured using the $^{11}\text{B}(^3\text{He},np)^{12}\text{C}$ reaction at low incident energies [2]. It has been found that the 15.06-MeV state has strong decays by proton emission to the 9.64-MeV, 3^- and 1083-MeV, 1^- states in ^{12}C , indicating the presence of configurations with two particles in the sd -shell orbitals. The Stanford group [3] studied proton decays from the excited states in ^{13}N . They detected decay protons in coincidence with emitted π^0 particles in the $^{13}\text{C}(\pi^+, \pi^0 p)^{12}\text{C}$ reaction, and reported that the analog giant resonance in ^{13}N mostly decays into the $T=1$ state in the daughter nucleus ^{12}C . Suzuki *et al.* [4] reported the measurement of neutron decay from the isovector giant

quadrupole resonance (IVGQR) in ^{13}C , which was excited by the $(e, e'n)$ reaction on ^{13}C . Neutron decay from ^{13}C should have a complete isobaric relation to proton decay from ^{13}N if we neglect the presence of the Coulomb force acting on the decay protons. They observed a strong neutron population to the $T=1$, 15.11 MeV 1^+ state in ^{12}C from the IVGQR in ^{13}C .

The $(^3\text{He},t)$ charge-exchange reaction at bombarding energies above 100 MeV/nucleon has several advantages such as (1) the relatively strong $V_{\sigma\tau}$ interaction at high energies, (2) a simple reaction mechanism, (3) a high resolution and high detection efficiency compared with those of (p,n) reactions, and (4) a large cross section of excitation of spin-flip states with a transferred angular momentum $\Delta L=0$. The advantages mentioned above enable us to measure decay particles in coincidence with high-energy tritons from the $(^3\text{He},t)$ reaction. Such coincidence experiments with proton decay have been performed successfully [5–7].

With the assumption of a direct charge-exchange reaction mechanism, simple arguments are possible to understand the excited states in ^{13}N . The ground state of ^{13}C has a main configuration with a $1p_{1/2}$ neutron above the ^{12}C core. The (p,n) and $(^3\text{He},t)$ reactions can excite states with configurations having one proton in the $1\pi p_{1/2}$ or sd -shell orbitals, one neutron in the $1\nu p_{1/2}$ orbit, and one neutron hole in the $1\nu p_{3/2}^{-1}$ orbit. When the charge-exchange reaction leads to one neutron hole in the ^{12}C core and one proton particle above

the $p_{3/2}$ orbit while leaving one $p_{1/2}$ neutron as a spectator, the Gamow-Teller ($\Delta L=0$) states and the spin-flip ($\Delta L=1$) dipole states are expected to be excited very strongly.

In recent publications [8–10], the 0^+ states at $E_x = 7.65$ MeV and $E_x \sim 10$ MeV in ^{12}C are discussed with the conjecture of three α -particle condensation. On the basis of this conjecture, Yamada *et al.* [11] suggest that the $1/2^-$ and $3/2^-$ states should appear as the spin-orbit partners with the $^{12}\text{C}(0^+) + N$ configuration in ^{13}C and ^{13}N . If the ground state of ^{13}C has a configuration with three α -cluster plus one neutron, the $^{13}\text{C}(^3\text{He}, t)^{13}\text{N}$ reaction is expected to lead to the excited $1/2^-$ and $3/2^-$ states in ^{13}N with such $^{12}\text{C}(0^+) + p$ configurations.

Thus, it is very interesting to study the proton decays from the $1/2^-$ and $3/2^-$ states in ^{13}N to the 0^+ states in ^{12}C . If the $1/2^-$ and $3/2^-$ states in ^{13}N have a strong configuration coupling with the 0^+ states in ^{12}C , some hints for such couplings would be found in the proton-decay measurements.

In the present paper, we report the results obtained from the singles measurement of the $^{13}\text{C}(^3\text{He}, t)^{13}\text{N}$ reaction at the intermediate energy of 450 MeV, and from the coincidence measurement in the $^{13}\text{C}(^3\text{He}, t-p)^{13}\text{N}$ reaction. The experimental angular distributions of the $(^3\text{He}, t)$ cross sections are compared with microscopic DWBA calculations. The branching ratios of proton decays are compared with the results of simple shell-model calculations for the excited states in ^{13}N .

II. EXPERIMENT

The experiments were carried out at the Research Center for Nuclear Physics (RCNP), Osaka University. The $^3\text{He}^{++}$ beam at 150 MeV/nucleon was obtained through the cascade acceleration with the $K=120$ MeV AVF cyclotron and the $K=400$ MeV ring cyclotron. The $^3\text{He}^{++}$ beam was transported to the target position with an achromatic beam-transport mode. Reaction products, tritons and ^3He , were momentum analyzed using the spectrometer “Grand Raiden” [12] and were measured with a focal-plane detection system.

The focal-plane detection system consisted of two sets of multiwire drift chambers (MWDC's) and two plastic scintillation counters. The ray-tracing technique with the MWDC's allowed us to obtain information on both the positions and the incidence angles of reaction ejectiles at the focal plane of the spectrometer. The plastic scintillators with a thickness of 5 mm were utilized for particle identification, for generating trigger signals, and for providing signals of stopping timing for the MWDC's.

Two ^{13}C targets were used in the experiment. One was a self-supporting ^{13}C foil with a thickness of 1.72 mg/cm² for proton-decay coincidence measurements. The energy resolution of the final states was determined by the energy loss of decay protons in the target used. Another target was a ^{13}C polyethylene foil with a thickness of 11 mg/cm² for singles measurements. The typical energy resolution [full width at half maximum (FWHM)] was 300 keV.

A. Singles measurements

The cross sections for the $^{13}\text{C}(^3\text{He}, t)^{13}\text{N}$ reaction were measured at $\theta_{\text{lab}} = 0^\circ - 17^\circ$. The cross sections for $^3\text{He} + ^{13}\text{C}$

elastic scattering were measured at $\theta_{\text{lab}} = 2^\circ - 14^\circ$. The opening angles, which were defined by the entrance slit of the spectrometer, were ± 10 mrad vertically and ± 20 mrad horizontally at $\theta_{\text{lab}} = 0^\circ$ and at $\theta_{\text{lab}} \geq 6^\circ$. At the scattering angles of $\theta_{\text{lab}} = 2^\circ - 4^\circ$, the slit set at ± 10 mrad was used only for defining the limitation of the vertical angle. The horizontal scattering angles were determined by the ray-tracing technique. The beam intensity was varied in the range between 3 and 15 nA, depending on the scattering angles and the type of measurements.

B. Coincidence measurements

Decay protons from the excited states in ^{13}N were measured in coincidence with tritons from the $(^3\text{He}, t)$ reaction. The spectrometer was set at 0° . The opening angles of the slits were set at ± 20 mrad horizontally and at ± 20 mrad vertically. The typical beam intensity was 4 nA, which was determined to achieve a good signal-to-noise ratio for the t - p coincidence measurements.

Decay protons from the excited states in ^{13}N were detected using an array of 40 lithium-drifted silicon detectors (SSD's) [13], which were mounted at backward angles with respect to the incident $^3\text{He}^{++}$ beam to reduce the nuclear continuum events which dominate at forward angles due to the quasifree processes with three-body final states. The SSD's were located at $\theta_{\text{lab}} = 100^\circ - 160^\circ$ with intervals of 10° .

The effective area of each silicon detector was about 450 mm². The thickness was 5 mm, enough to stop decay protons with an energy up to $E_p = 30$ MeV. The distance between the target and the front surface of each detector was 150 mm. The total solid angle for proton detection covered by the SSD array was 5.7% of 4π .

The frame of the SSD's array was copper plate with a thickness of 2 mm, which was connected to a copper cooling pipe. The SSD's were cooled down to -25°C by circulating ethylene-glycol liquid to reduce the thermal noise of SSD's and to improve the resolution. Each SSD was electrically insulated by ceramic plates to reduce the noise.

III. RESULTS AND DISCUSSION

A. Singles spectra

Figure 1 shows the $^{13}\text{N}(^3\text{He}, t)^{13}\text{C}$ singles spectra at $\theta_{\text{lab}} = 0^\circ, 2.25^\circ, 6.25^\circ$, and 8.75° . In the 0° spectrum, we observed several discrete states with the transferred angular momentum of $\Delta L=0$. The excitation energies and J^π values for these states are labeled in Fig. 1(a). In the spectra at large scattering angles, other discrete states with $\Delta L \geq 1$ were prominently excited. These states are indicated by the arrows in Fig. 1. In Fig. 1(b), the 2.36-MeV $1/2^+$, 6.36-MeV $5/2^+$, and 6.89-MeV $3/2^+$ states are indicated as those excited with the transferred angular momentum of $\Delta L=1$. At 6.25° , the 7.38-MeV $5/2^-$, 16-MeV, and 21-MeV states have been observed as those with $\Delta L=2$.

As seen in Fig. 1(b), some broad peaks have been observed at excitation energies, $E_x \geq 16$ MeV. These broad peaks are inferred to be due to the excitation of spin-dipole

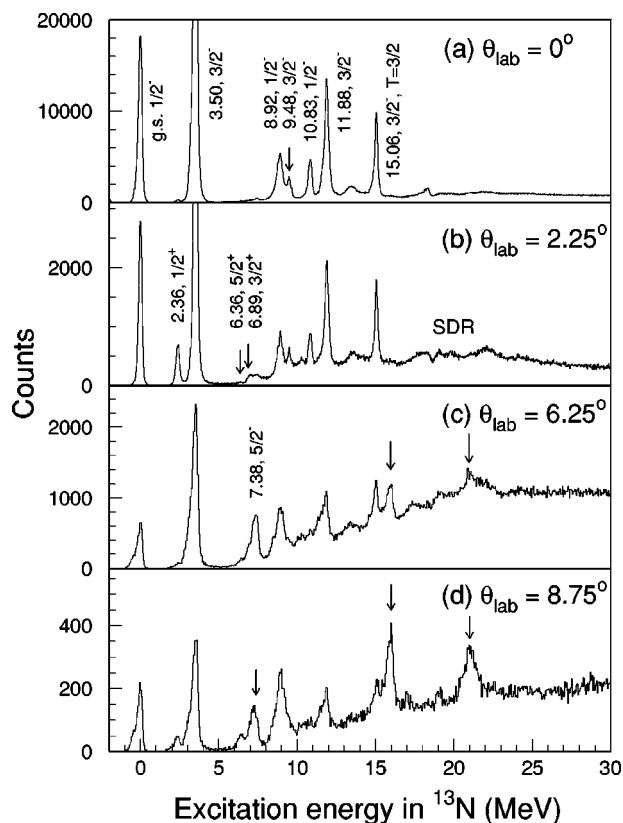


FIG. 1. Singles energy spectra of the $^{13}\text{C}(^3\text{He}, t)^{13}\text{N}$ reaction at $E(^3\text{He})=450$ MeV and at $\theta_{\text{lab}}=0^\circ$, 2.25° , 6.25° , and 8.75° .

resonances (SDR's) with $\Delta L=1$. These broad peaks are superimposed on a nonresonant continuum from the quasifree three-body processes. This becomes dominant at large scattering angles.

Table I lists the discrete states in ^{13}N observed in the present $(^3\text{He}, t)$ measurements. These are compared with the previous experimental results taken from Ref. [14]. In order

to determine the cross sections of the discrete states, we first fitted the peak shapes. In the case that the widths of the states were very narrow, compared with the resolution of the present experiment, and the excitation energies were well known, we used the widths taken from Ref. [14] in the spectrum fitting procedure except for the states at $E_x=10.83$, 11.74 , and 16 MeV.

Since the proton-separation energy of ^{13}N is very low, $S_p=1.9435$ MeV, all the excited states have intrinsic natural widths. Thus, Lorentzian shapes were employed in fitting the peak shapes of the discrete states. When the beam resolution of 300 keV was not negligibly small compared with the width of a discrete state, the Lorentzian shapes were folded with the beam resolution. The background shape was assumed to be fitted with a second-order polynomial function and the shapes of the discrete states were not affected by the choice of the function for the background shapes.

Although the width of the 10.83 -MeV $1/2^-$ state was not been obtained in previous work, the peak shape for this state was found to be sharp compared with that of the 11.88 -MeV state. In the peak fitting process with the Lorentzian shape, the level widths for the 10.83 - and 11.88 -MeV states were set as free parameter. The width of the 10.83 -MeV state obtained in this fitting was almost zero. From its angular distribution, the 11.88 -MeV state in ^{13}N is inferred to be excited with $\Delta L=0$. This state corresponds to the $3/2^-$ state at $E_x=11.74$ MeV reported in Ref. [14]. The width of 98 keV obtained for this state is smaller than the values of 530 ± 80 keV given in Ref. [14].

Figure 2 shows the high-excitation energy parts of the $^{13}\text{C}(^3\text{He}, t)^{13}\text{N}$ spectra at $\theta_{\text{lab}}=0^\circ$, 2.25° , and 6.25° . We observed several broad peaks (resonances) above the excitation energy of 16 MeV. These peaks are well observed at backward angles, and are inferred to correspond to the SDR's with $\Delta L=1$. Yang *et al.* [15] have reported the results of the multipole decomposition analysis for the $^{13}\text{C}(p, n)^{13}\text{N}$ reaction at $E_p=186$ MeV to obtain $\Delta L=1$ strengths. They found that a considerable amount of $\Delta L=1$ strengths exists at E_x

TABLE I. Excitation energies and widths of the discrete states in ^{13}N .

Ex (MeV) ^a	J^π, T	Γ (keV) ^a	Ex (MeV) ^b	Γ (keV) ^b
0.0	$1/2^-; 1/2$	$\tau_{1/2}=9.965 \pm 0.004$ min		
2.3649 ± 0.0006	$1/2^+$	31.7 ± 0.8		
3.502 ± 0.002	$3/2^-$	62 ± 4		
6.364 ± 0.009	$5/2^+$	11		
6.886 ± 0.008	$3/2^+$	115 ± 5		
7.155 ± 0.005	$7/2^+$	9 ± 0.5		
7.376 ± 0.009	$5/2^-$	75 ± 5		
8.918 ± 0.011	$1/2^-$	230		
9.476 ± 0.008	$3/2^-$	30		
10.833 ± 0.009	$1/2^-$			
11.74 ± 0.009	$3/2^-$	530 ± 80	11.88	98.0
15.06457 ± 0.0004	$1/2^-; 3/2$	0.86 ± 0.12	16.0	163.0

^aReference [14].

^bDetermined by fitting present experimental data.

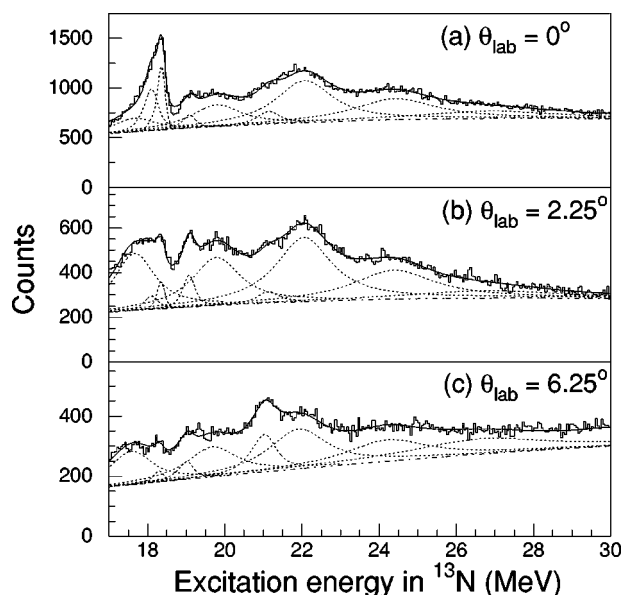


FIG. 2. The $^{13}\text{C}(^3\text{He}, t)^{13}\text{N}$ energy spectra at $\theta_{\text{lab}} = 0^\circ$, 2.25° , and 6.25° . The dotted lines show the results of peak fitting. The dash-dotted lines show the background shape due to the quasifree processes. The solid lines are the superposition of peak fitting and the assumed background.

$= 10 \sim 30$ MeV, making the SDR in ^{13}N . When we compared the (p, n) and $(^3\text{He}, t)$ spectra, we noticed that the shape of the (p, n) spectrum [see Fig. 1(f) in Ref. [15]] and the $(^3\text{He}, t)$ spectrum at $\theta_{\text{lab}} = 2.25^\circ$ are rather similar and the bump corresponding to the SDR's consists of many broad peaks.

To extract the shapes of the broad peaks, the nonresonant continuum was subtracted. The nonresonant background from the quasifree three-body processes was assumed to be described by a semiphenomenological function based on the Fermi-gas model developed by Erell *et al.* [16] for fitting the spectrum shape obtained in the (π^\pm, π^0) reactions. In this procedure, the quasifree continuum was assumed to have a Lorentzian shape with an exponential cutoff that simulates the Pauli blocking effect at the low-excitation-energy side. The parameters for fitting the shape of the quasifree continuum were taken from Ref. [17].

The shape of the broad peaks was assumed to be a Lorentzian shape. The widths and the excitation energies of these peaks were determined by fitting these three spectra simultaneously. The results are listed in Table II. It is very difficult to find the one-to-one correspondence between the obtained resonance locations and those tabulated in the compilation work by Ajzenberg-Selove [14]. However, it is worthy to note that the global shape of the $^{13}\text{C}(^3\text{He}, t)^{13}\text{N}$ spectrum at $\theta_{\text{lab}} = 2.25^\circ$, where the spin dipole resonance (SDR) is expected to be strongly excited, is mainly fitted with the four broad bumps at $E_x = 17.68$, 19.83 , 22.14 , and 24.50 MeV.

B. Angular distribution of Gamow-Teller (GT) states

Cross sections for the $^{13}\text{C}(^3\text{He}, t)^{13}\text{N}$ reaction at 450 MeV were calculated in the framework of the distorted-wave Born

TABLE II. Excitation energies and widths of excited states observed in ^{13}N above $E_x = 16$ MeV.

E_x (MeV)	Γ (keV)
17.68 ± 0.03	1212 ± 74
18.12 ± 0.02	276 ± 41
18.37 ± 0.01	23
19.11 ± 0.01	183 ± 41
19.83 ± 0.02	1542 ± 84
21.20 ± 0.01	581 ± 44
22.14 ± 0.01	1706 ± 82
24.50 ± 0.04	2466 ± 218
26.9 ± 0.9	4380 ± 470

approximation (DWBA) using the code DWBA98 [18]. The transition densities used were calculated with the code OXBASH [19]. The Cohen and Kurath two-body interaction (CKII) [20] was used for the $0\hbar\omega$ $1p \rightarrow 1p$ transitions. For calculations in both the $0\hbar\omega$ and $2\hbar\omega$ spaces, the Warburton and Brown (WBT) [21], and the Millener-Kurath interaction (PSDMK2) [22], those taken from the recent work by Otsuka (PSDMK2 No. 1 [23]), and those by Suzuki (PSDMK2 No. 2) [24] were used. The single-particle states were calculated in the Saxon-Woods potential. Using the elastic scattering data measured in the present work, the $^3\text{He} + ^{13}\text{C}$ optical-potential parameters based on the Saxon-Woods parameterization were obtained with the code ECIS79 [25]. The obtained parameters are $V_r = 19.07$ MeV, $r_o = 1.554$ fm, $a_v = 0.696$ fm, $V_i = 35.98$ MeV, $r_i = 0.937$ fm, and $a_i = 0.860$ fm. Figure 3 shows the comparison between the results of the optical-model calculation and the experimental angular distribution for the $^3\text{He} + ^{13}\text{C}$ elastic scattering. The reduced χ^2 value for the best-fit parameters was 2.46. For tritons, the optical-potential parameters were assumed to be similar or equal to the ^3He parameters. However, the potential-well depths were taken 85% of the depths for the ^3He particles. For the $(^3\text{He}, t)$ reactions at the bombarding energies of 60–90, 177, and 410 MeV, it was found that by taking the well depths of the optical potential for the outgo-

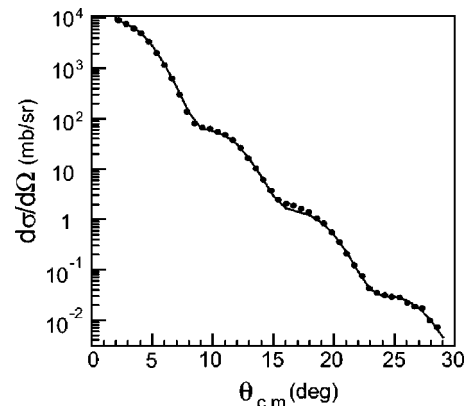


FIG. 3. Experimental angular distribution of the $^3\text{He} + ^{13}\text{C}$ elastic scattering at $E(^3\text{He}) = 450$ MeV. The experimental data are compared with the result of the optical-model calculation.

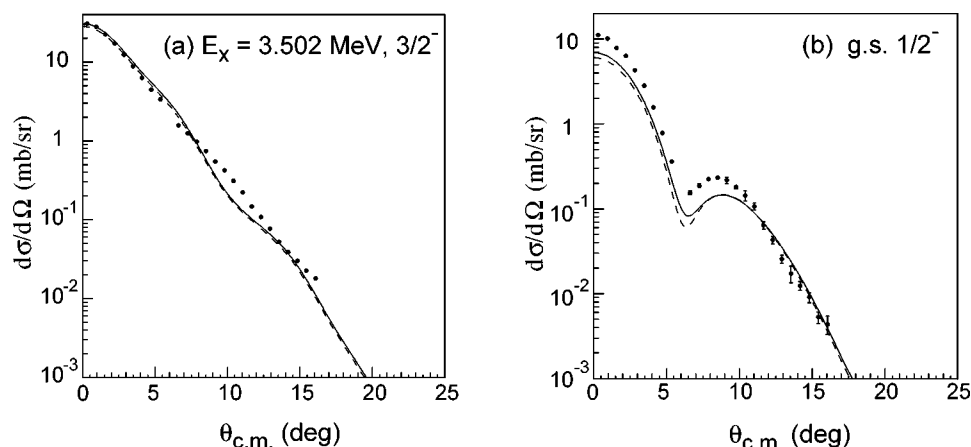


FIG. 4. Experimental differential cross sections and the results of DWBA calculations. The solid curves are the results of the DWBA calculations with the transition densities obtained using the Cohen and Kurath two-body interactions. The dashed curves are those with the WBT transition densities. (a) The cross sections for the $^{13}\text{C}(^3\text{He},t)^{13}\text{N}(3.50\text{-MeV}, 3/2^-)$ reaction. (b) The cross sections for the $^{13}\text{C}(^3\text{He},t)^{13}\text{N}(\text{g.s.}, 1/2^-)$ reaction.

ing triton channel 85% of the incoming ^3He channel and by keeping the other parameters equal to the ^3He parameters, good fits for the angular distributions of the $(^3\text{He}, t)$ reactions were achieved [26–28].

An effective ^3He -nucleon interaction can be obtained, in principle, by folding the effective NN interaction over the ^3He ground-state density. Using a form similar to the isovector part of the NN interaction with one range for each component, while the effective NN interaction has three or four ranges for each component, the cross sections of the $^{42}\text{Ca}(^3\text{He}, t)^{42}\text{Sc}$ reaction at 30 MeV were microscopically well described in DWBA as a one-step process [29]. In this calculation, the various interaction terms were represented with Yukawa shapes with the ranges of $R_\tau = R_{\sigma\tau} = 1.415$ fm and $R_{T\tau} = 0.878$ fm, for the isospin (V_τ), spin-isospin ($V_{\sigma\tau}$), and tensor ($V_{T\tau}$) interactions. This ^3He - n force was also used at 66–90 MeV to describe the $(^3\text{He}, t)$ reaction cross sections for several target nuclei [26]. In spite of the fact that the energy of 90 MeV is about three times higher than 30 MeV, the procedure mentioned above was found to be successful in quantitatively describing the cross sections of the various multipole excitations. As a first trial, we used the effective ^3He - n interaction at 450 MeV with the same form and the same ranges that were used at lower incident energies.

At scattering angles around 0° , GT transitions ($\Delta T = 1, \Delta L = 0, \Delta S = 1$) are mainly mediated by $V_{\sigma\tau}$ and Fermi transitions ($\Delta T = 1, \Delta L = 0, \Delta S = 0$) are mediated by V_τ . By fitting the angular distributions of the pure GT transitions in ^{13}N , we defined the strength of the isovector central term $V_{\sigma\tau}$. Since the J^π transfer in the $^{13}\text{C}(1/2^-) \rightarrow ^{13}\text{N}(3.50\text{-MeV}, 3/2^-)$ reaction is 1^+ , it is enough to take into account only the $V_{\sigma\tau}$ component. Figure 4(a) shows the experimental differential cross sections for the 3.50-MeV $3/2^-$ state in ^{13}N in comparison with the results of DWBA calculations. In the DWBA calculations, the effective interaction $V_{\sigma\tau}$ was assumed to have a Yukawa-shape function with a range of $R_{\sigma\tau} = 1.415$ fm which was the same as those used at lower bombarding energies. In the calculations, two types of wave functions were used: One was obtained with the Cohen and Kurath two-body interactions (CKII) in the $0\hbar\omega$ space and the other was with the WBT in the $2\hbar\omega$ space. Both results of the DWBA calculations were found to agree well with each other. The calculated results with the other transition

densities [not plotted in Fig. 4(a)] were only slightly different from those with the CKII and WBT. From the comparison with the data, we conclude that a $V_{\sigma\tau}$ value of -3.0 MeV is appropriate for the DWBA calculations to describe the $^{13}\text{C}(^3\text{He}, t)$ results.

There is no pure Fermi transition in the case of the $^{13}\text{C}(^3\text{He}, t)^{13}\text{N}$ reactions since the $\Delta L = 0$ transition from the $1/2^-$ ground state of ^{13}C to the $1/2^-$ analog ground state of ^{13}N is allowed both with $\Delta J^\pi = 0^+$ and 1^+ . Both the Fermi and GT transitions contribute to the cross section for the $^{13}\text{C}(1/2^-) \rightarrow ^{13}\text{N}(1/2^-, \text{g.s.})$ transition at $\theta_{\text{lab}} \sim 0^\circ$. In the present work, the strength V_τ was determined using the ratio of the volume integrals of the effective interactions $|J_\tau/J_{\sigma\tau}|^2$. With the value of $|J_\tau/J_{\sigma\tau}|^2 = 0.12 \pm 0.01$ [30,31], the V_τ value was set at 1.039 MeV. To check the validity of the values of V_τ and $V_{\sigma\tau}$, the DWBA calculation for the $^{13}\text{C}(^3\text{He}, t)^{13}\text{N}(\text{g.s.})$ reaction has been performed. Figure 4(b) compares the results of the DWBA calculations and the experimental angular distributions. The shape of angular distribution near 0° agrees with the experimental data. The magnitude of calculated differential cross section is, however, a factor of 2 smaller than the experimental data.

From the NN t -matrix interaction, it is known that the range of the central terms has three or four components to describe the long- and short-range parts due to the one-pion-exchange process (OPEP) and due to the heavy-meson exchanges. The ranges in the Yukawa functions have been chosen to reproduce the long-range OPEP behavior of the force. At low bombarding energies, the short-range components arising from ρ -meson or two-pion exchange in the NN force are smeared out and give rise to the ranges close to the OPEP values when the relevant components are averaged over the volume of the ^3He particle. On the other hand, at higher bombarding energies such as 150 MeV/nucleon, we may need to add components of shorter ranges to the effective ^3He - n force. This is especially true in the case of the Fermi transition, which is primarily associated with the two-pion and heavy meson exchange processes.

To see the necessity of shorter ranges, the DWBA calculation with transition densities obtained using the WBT interaction in the $2\hbar\omega$ space was performed with ranges R_τ shorter than 1.415 fm. For simplicity, only the range of V_τ was replaced to shorter one and the strength was calculated to keep the constant ratio of the volume integral of

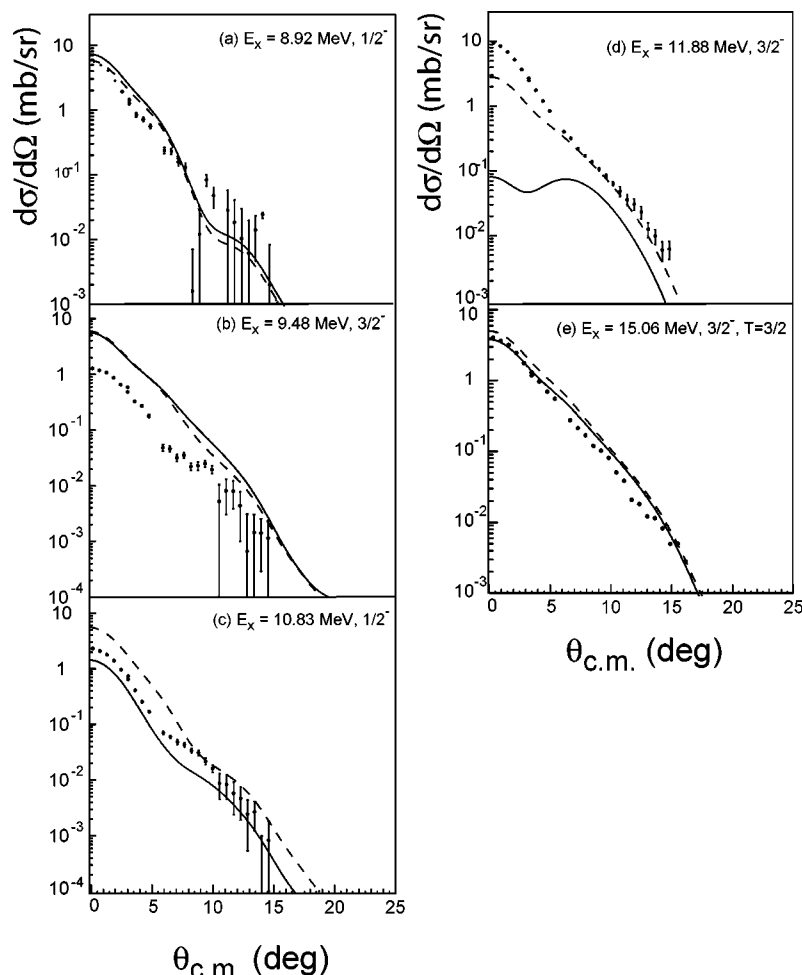


FIG. 5. Experimental cross sections and the results of DWBA calculations. The solid curves are the results with the Cohen and Kurath transition densities in the $0\hbar\omega$ space. The dashed curves are the results with the WBT transition densities in the $2\hbar\omega$ space.

$|J_\tau/J_{GT}|^2 = 0.12$. Assuming of $R_\tau = 0.4$ fm, the magnitude V_τ becomes 45.92 MeV, and in the case of $R_\tau = 0.2$ fm, V_τ is 358 MeV. The changes of the shapes of the calculated angular distribution were very small near 0° even if we used the different ranges. The change in magnitude of the calculated differential cross section was also small near 0° and there was no drastic change in the angular distribution.

The difficulty of describing the $^{13}\text{C}(1/2^-, \text{g.s.}) \rightarrow ^{13}\text{N}(1/2^-, \text{g.s.})$ transition in the DWIA calculation has already discussed by Wang *et al.* [32,33] using cross sections and complete sets of polarization-transfer coefficients. Wang *et al.* [33] used the normalization factor for the GT component in adjusting the absolute cross sections. Similar renormalization processes may be needed to obtain an agreement between the $^{13}\text{C}(^3\text{He}, t)^{13}\text{N}(\text{g.s.})$ cross section and the DWBA calculation. However, reexamination of the used wave functions in describing the ground states of ^{13}C and the states in ^{13}N would be needed at first.

The angular distributions of the GT states at $E_x = 8.92$, 9.48, 10.83, 11.88, and 15.06 MeV are shown in Fig. 5. We found that the shapes of the experimental differential cross sections of the GT states are much the same. The shapes of the present DWBA calculations, however, were not the same, especially for the 11.88-MeV $3/2^-$ state when we used the Cohen and Kurath wave function. This disagreement between the experimental data and the DWBA calculation

might be due to the incorrectness of the wave function calculated with the two body interactions. On the other hand, Yamada *et al.* [11] recently discussed that the $1/2^-$ and $3/2^-$ states in ^{13}N result from the $^{12}\text{C}(0_1^+) + p$ configurations. Thus, it is interesting to discuss the structures of the observed $1/2^-$ and $3/2^-$ states at $E_x < 15$ MeV from the clustering aspect.

C. Coincidence spectra

Figure 6(a) shows a two-dimensional scatter plot of proton energy versus $E_x(^{13}\text{N})$ for t - p coincidence events induced by the $^{13}\text{C}(^3\text{He}, t)^{13}\text{N}$ reaction at 0° . A 0° singles ($^3\text{He}, t$) spectrum, which has been measured at the same time, is compared with the two-dimensional scatter-plot of decay protons [Fig. 6(b)] for easy reference. For proton-decay from an excited state in ^{13}N , the energy E_f of the final state in ^{12}C is given as

$$E_f = E_x(^{13}\text{N}) - E_p - S_p - E_{\text{recoil}}, \quad (1)$$

where E_{recoil} , E_p , and S_p are the recoil energy of the ^{12}C nucleus, the kinetic energy of decay proton, and proton separation energy, respectively. The loci for proton decay from the excited states in ^{13}N to the 0_1^+ ground, 4.44-MeV 2^+ , 7.65-MeV 0_2^+ , 12.71-MeV 1^+ , and 15.11-MeV 1^+ $T=1$, 16.11-MeV 2^+ $T=1$ states in ^{12}C are clearly identified as lines corresponding to $E_x(^{13}\text{N}) - E_p = \text{const}$. The proton and

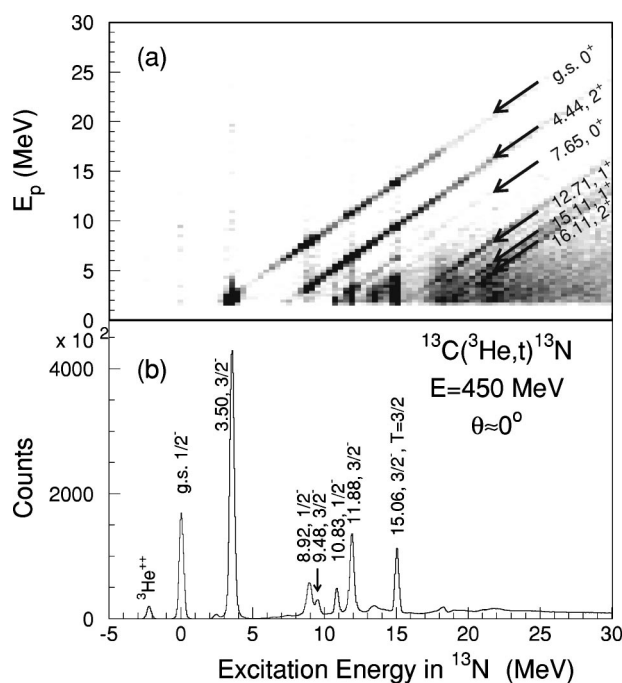


FIG. 6. (a) Two-dimensional scatter plot of proton-triton coincidence events induced by the $^{13}\text{C}(^3\text{He},t)^{13}\text{N}$ reaction at 150 MeV/nucleon and at $\theta_{\text{lab}} \sim 0^\circ$. The loci indicate proton-decay events from the excited states in ^{13}N to the final states in ^{12}C . (b) Singles spectrum of the $^{13}\text{C}(^3\text{He},t)^{13}\text{N}$ reaction at $\theta_{\text{lab}} \sim 0^\circ$.

neutron separation energies of ^{13}N are $S_p=1.9435$ MeV and $S_n=20.064$ MeV, respectively. Thus, proton decay from the excited states in ^{13}N dominates at excitation energies between S_p and S_n since the probabilities of α and deuteron emissions are relatively low. It should be noted here that proton-decay events with energies lower than $E_p \sim 12$ MeV were cut off by an electronic threshold in the present experiment.

The discrete final states in ^{12}C are seen in Fig. 7, which has been obtained by projecting the two-dimensional scatter plot onto the excitation energy axis of ^{12}C . As shown in Fig. 7(a), the states in ^{13}N with excitation energies lower than $E_x=15.06$ MeV mostly decay by proton emission to the 0_1^+ and 2_1^+ states in ^{12}C . It is interesting to point out that the 7.65-MeV 0_2^+ state in ^{12}C is mainly fed by proton emission from the states at $E_x=10-15.06$ MeV. Figure 7(b) shows the final-state spectrum for proton decay from highly excited continuum states in ^{13}N to the ground state and the low-lying states in ^{12}C as well as to higher discrete excited states in ^{12}C . A characteristic feature of the final-state spectrum in Fig. 7(b) is the fact that the broad resonances at high excitation energies in ^{13}N decay by proton emission into the highly excited states in ^{12}C .

Figures 8 and 9 show the coincidence $^{13}\text{C}(^3\text{He},tp)$ energy spectra in ^{13}N , which are again compared with the singles $^{13}\text{C}(^3\text{He},t)^{13}\text{N}$ spectrum [Fig. 8(a)] for easy reference. Each coincidence spectrum is obtained by gating the decay-proton events to the final discrete states in ^{12}C . In the t - p coincidence spectrum for the events to the ground state of ^{12}C [Fig. 8(b)], we observe that the proton decay from the 10.83-MeV $1/2^-$ state in ^{13}N to the ground state of ^{12}C is strongly

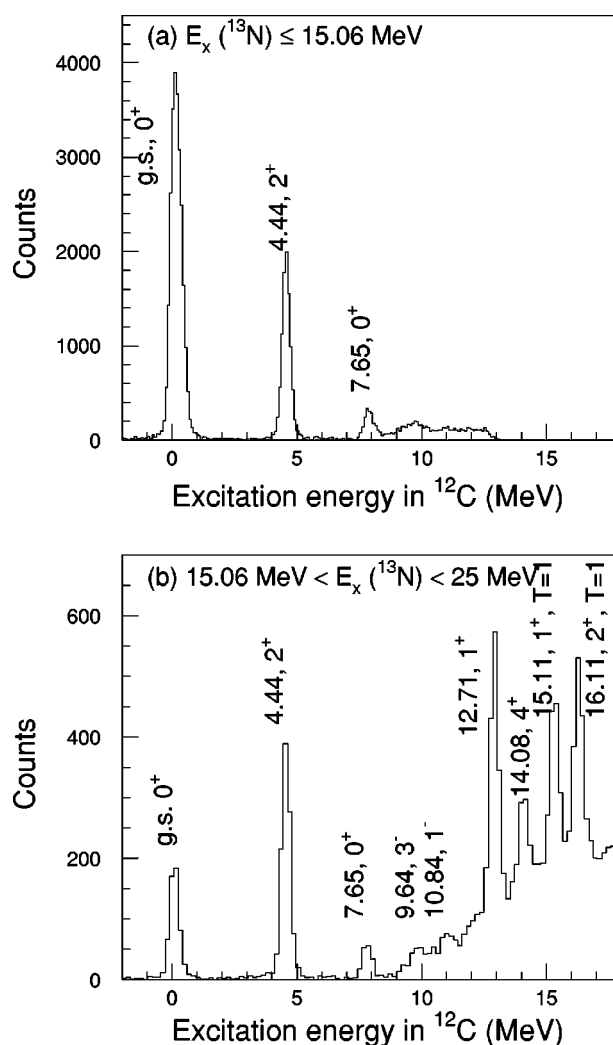


FIG. 7. Final-state spectra of ^{12}C after proton decay (a) from the states in the excitation energy region of $E_x \leq 15.06$ MeV in ^{13}N where GT states are mainly excited and (b) from the states at $15.06 \text{ MeV} < E_x < 25.0$ MeV in ^{13}N where the SDR region is mainly excited.

suppressed, while the proton decay from the same 10.83-MeV state to the 4.44-MeV 2_1^+ and 7.65-MeV 2_2^+ states in ^{12}C are clearly observed [see Figs. 8(c) and 8(d)]. This suppression is qualitatively interpreted in the framework of the shell-model calculations and is discussed in detail later.

As indicated in Fig. 8(b), proton-decay events in the continuum region suddenly decrease above the threshold energy of the $^{11}\text{C}+d$ decay ($S_d=18.44$ MeV). This decrease of proton-decay events is not recognized, for example, in Fig. 8(c). It is well known that when the neutron-decay channel opens, other decay channels by charged-particle emission are suppressed because of a high probability of neutron emission. However, the probability of deuteron emission is not higher than that of proton emission. Thus, the present observation remains as an unanswered question and requires a special enlarged deuteron-decay channel near the threshold.

The 15.06-MeV $3/2^-$ $T=3/2$ state decays to the $T=0$ states in ^{12}C [see Figs. 8(b)–8(d)]. On basis of the isospin selection rule that the isospin is conserved as a good quan-

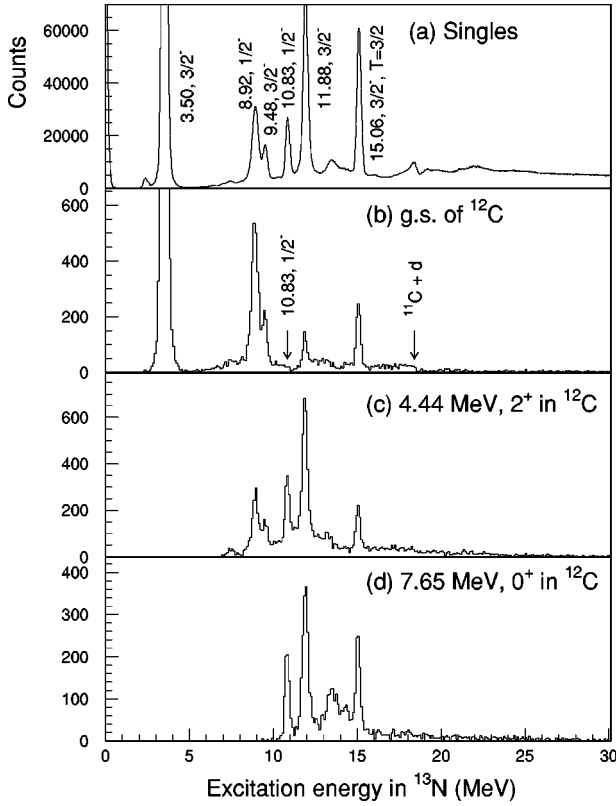


FIG. 8. Comparison between the $^{13}\text{C}(^3\text{He},t)^{13}\text{N}$ singles spectrum (a) and the spectra obtained with the t - p coincidence gates. Both the singles $^{13}\text{C}(^3\text{He},t)^{13}\text{N}$ spectrum and the t - p coincidence spectra have been obtained at $\theta_{\text{lab}}=0^\circ$. The coincidence energy spectra in ^{13}N have been obtained by projecting the event loci for decay protons to the three final states in ^{12}C : (b) the ground state, (c) the 4.44-MeV 2^+ state, and (d) the 7.65-MeV 0^+ state.

tum number in the system, proton decay from the pure $T=3/2$ states to the $T=0$ states is forbidden because the decay proton carries only the isospin $\Delta T=1/2$. Thus, we can conclude that the 15.06-MeV state has a considerable amount of the isospin violation component in the wave function, surpassing the weak γ -decay rates.

In the t - p coincidence spectra obtained by gating on the proton-decay events to the higher excited states in ^{12}C , we observed some sharp peaks, which are indicated by arrows at $E_x=17$ and 19 MeV in Figs. 9(b) and 9(c), and $E_x=21$ and 22.5 MeV in Figs. 9(c) and 9(d), respectively. These new sharp peaks have never been reported in previous works on the singles measurements. These states in ^{13}N could be the isobaric analog states of the excited states in ^{13}C with isospin $T=3/2$.

D. Branching ratio

The escape width Γ is expressed as the sum of the proton partial escape widths Γ_i to the final nuclei since decay by γ -ray emission is negligibly smaller than that by proton emission. The escape width is written as

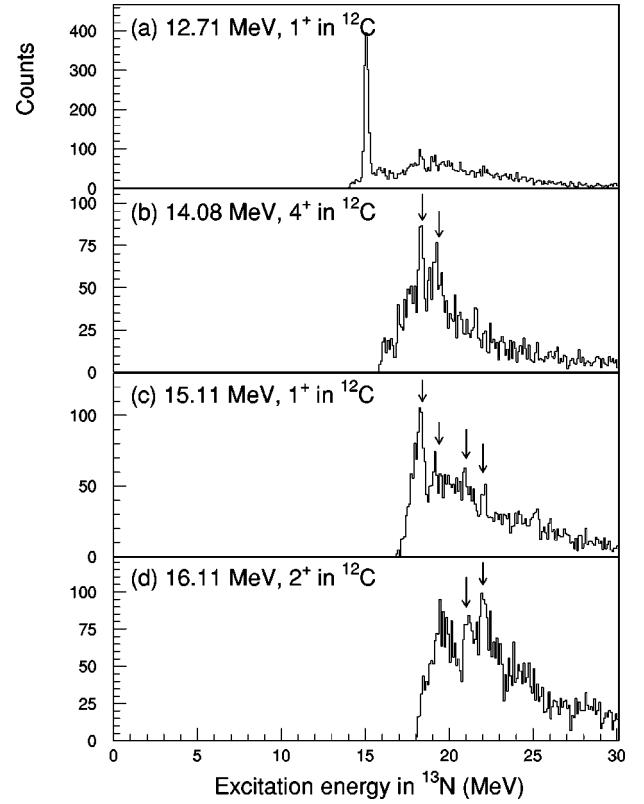


FIG. 9. The t - p coincidence spectra in ^{13}N obtained by projecting the event loci to the four final states in ^{12}C : (a) the 12.71-MeV 1^+ state, (b) the 14.08-MeV 4^+ state, (c) the 15.11-MeV 1^+ $T=1$ state, and (d) the 16.11-MeV 2^+ $T=1$ state. The arrows indicate the discrete states at $E_x=17$, 19, 21, and 22.5 MeV, which could be the isobaric analog states in ^{13}C with $T=3/2$.

$$\Gamma = \sum_i \Gamma_i. \quad (2)$$

The branching ratio defined by the partial escape width divided by the total width is expressed in terms of the coincidence double-differential cross section to the singles cross section

$$\frac{\Gamma_i}{\Gamma} = \int \frac{d^2\sigma_i(\theta, \phi)}{d\Omega_t d\Omega_p} d\Omega_p \bigg/ \frac{d\sigma}{d\Omega_t}. \quad (3)$$

The experimental branching ratios for proton decay from the states in ^{13}N to the final states in ^{12}C are summarized in Table III.

The 3.50-MeV $3/2^-$ state in ^{13}N decays by proton emission only to the ground state (g.s.) in ^{12}C . Therefore, the branching ratio from the 3.50-MeV state to the ^{12}C g.s. should be nearly 1. However, the result obtained in the present experiment was 0.71 ± 0.17 , which was much lower than 1.0. This is due to the inefficiency of proton detection due to the energy loss of the low-energy decay protons in the carbon target depending on the emission angle and the reaction position of proton; the detection efficiency of low-energy decay protons decreases near the electronic threshold [see Fig. 6(a)]. In the case of the detection of proton decay from the 3.50-MeV $3/2^-$ state, the energy of decay protons

TABLE III. Branching ratios for proton decay from the GT states in ^{13}N . The uncertainties of the effective area of SSD are included in the errors of the present measurements.

E_x in ^{13}N (MeV)	E_x in ^{12}C		
	0.0 (0^+)	4.42(2^+)	7.65(0^+)
3.50($3/2^-$)	0.71 \pm 0.17		
8.92($1/2^-$)	0.60 \pm 0.09	0.30 \pm 0.05	
9.48($3/2^-$)	0.58 \pm 0.11	0.43 \pm 0.09	
10.83($1/2^-$)	0.05 \pm 0.01	0.54 \pm 0.09	0.43 \pm 0.16
11.88($3/2^-$)	0.08 \pm 0.01	0.35 \pm 0.05	0.10 \pm 0.02
15.06($3/2^-$)	0.16 \pm 0.02	0.13 \pm 0.02	0.03 \pm 0.01

was not high enough to correctly accumulate all the decay events and the branching ratio obtained became less than 1. The total branching ratio from the 11.88-MeV $3/2^-$ state is also less than 1. Since only proton decay occurs from this state, the total branching ratio to the ground, 4.44-MeV 2^+ , 7.65-MeV 0^+ states should be 1. The reason why the total branching ratio is less than 1 has not yet been understood.

In the resonance scattering of the $^{12}\text{C}(p,p')^{12}\text{C}^*$ reaction, proton decays from the 15.06-MeV $3/2^-$, $T=3/2$ state in ^{13}N to the final states in ^{12}C have already been measured [14]. The branching ratios of proton decays reported are 0.228 \pm 0.016 to the 0^+ g.s., 0.140 \pm 0.014 to the 4.44-MeV 2^+ state, and 0.049 \pm 0.015 to the 7.65-MeV 0^+ state in ^{12}C , respectively. The present branching ratios of proton decays from the 15.06-MeV state agree with these values reasonably well (see Table III).

The branching ratios of direct proton decay for various channels depend on the penetrability of the Coulomb and centrifugal barriers as well as the nuclear wave functions. The branching ratios are written as

$$\frac{\Gamma_i}{\Gamma} = \frac{\sum_{n,l,j} S(n,l,j)_i T_{lj}(E_x)}{\sum_i \sum_{n,l,j} S(n,l,j)_i T_{lj}(E_x)}, \quad (4)$$

where $S(n,l,j)$ and T_{lj} are the spectroscopic factor and the transmission coefficient, respectively. The transmission coefficients were calculated using the code ECIS79. The optical potential used was taken from Ref. [34]. The spectroscopic factors were calculated with the code OXBASH [19]. The two-body interactions used were taken from the works of Cohen and Kurath (CKII) [20], WBT [21], PSDMK2 [22], Otsuka *et al.* [23], and Suzuki [24]. The shell-model calculations were performed in the $0\hbar\omega$ space for the interaction of Cohen and Kurath, and in the $2\hbar\omega$ space for the other four interactions. The experimental branching ratios are listed in Table IV, and are compared with the results of the calculations. It should be noted that the theoretical results are normalized to make the proton decay branching ratio $\sum \Gamma_i/\Gamma \sim 1$, for easy comparison between the experimental branching ratios and the theoretical results. The calculations for the proton decay from the 15.06-MeV $3/2^-$ $T=3/2$ state to the low-lying $T=0$ states in ^{12}C were not performed since the proton decay from the $T=3/2$ states to the $T=0$ state is isospin forbidden and since the isospin violation is not taken into account in the shell-model calculations.

From the comparison between the experimental results and the calculations shown in Table IV, we can easily judge the validity of the theoretical calculations to give a better description for the proton decay data. For the 8.92-MeV $1/2^-$ state in ^{13}N , the branching ratios calculated by using the two-body interactions of Otsuka *et al.* [23] and Suzuki [24] are similar, and well reproduce the experimental branching ratios. For the 9.48-MeV $1/2^-$ and the 10.83-MeV $3/2^-$ states in ^{13}N , the branching ratios with WBT [21] are rather

TABLE IV. The $S(n,j,l)T_l$ values. Spectroscopic factors $S(n,j,l)$ are calculated using the code OXBASH. Transmission coefficients T_l are calculated using the code ECIS79 with the Perey and Perey optical potential [34]. The shell-model calculations are performed in the $0\hbar\omega$ space for Cohen and Kurath (CKII) interaction [20], and in the $2\hbar\omega$ space for the Warburton and Brown (WBT) [21], the Millener-Kurath interaction (PSDMK2) [22], those taken from the recent work by Otsuka (PSDMK2 No. 1 [23]) and those by Suzuki (PSDMK2 No. 2 [24]).

^{13}N state Ex (MeV)	^{12}C state Ex (MeV)	Theory					
		experiment	CKII	WBT	PSDMK2	PSDMK2 No. 1 ^a	PSDMK2 No. 2 ^b
8.92($1/2^-$)	0.00(0^+)	0.60 \pm 0.09	0.33	0.56	0.32	0.64	0.69
	4.44(2^+)	0.30 \pm 0.05	0.67	0.45	0.68	0.36	0.31
9.48($3/2^-$)	0.00(0^+)	0.58 \pm 0.11	0.95	0.47	0.78	0.24	0.15
	4.44(2^+)	0.43 \pm 0.09	0.05	0.53	0.22	0.76	0.85
10.83($1/2^-$)	0.00(0^+)	0.05 \pm 0.01	0.06	0.14	0.09	0.18	0.10
	4.44(2^+)	0.54 \pm 0.09	0.60	0.54	0.59	0.34	0.37
	7.65(0^+)	0.43 \pm 0.16	0.34	0.33	0.32	0.47	0.52
11.88($3/2^-$)	0.00(0^+)	0.08 \pm 0.01	0.03	0.13	0.13	0.12	0.17
	4.44(2^+)	0.35 \pm 0.05	0.44	0.28	0.32	0.50	0.29
	7.65(0^+)	0.10 \pm 0.02	0.52	0.59	0.55	0.38	0.54

^aTwo-body interaction for S_{njl} from the work by Otsuka *et al.* [23].

^bTwo-body interaction for S_{njl} from the work by Suzuki [24].

similar to the experimental results. The experimental branching ratios for the 11.88-MeV $3/2^-$ state in ^{13}N are not reproduced in any calculations. The 7.65-MeV 0_2^+ state in ^{12}C is well known to have a considerable amplitude of the α -cluster wave function. The branching ratios to this 0^+ state calculated in the shell-model framework are considerably higher than the experimental value.

At the present stage, we conclude that there is no two-body interaction which can reproduce the branching ratios of all the GT states consistently. Therefore, more sophisticated theoretical calculations are inevitable to describe the proton decay data. In other words, it is fair to say that the proton-decay data obtained in the present experiment serve as a stringent test for the microscopic structure of the excited states both in ^{13}C and ^{13}N .

IV. SUMMARY

The spin-isospin excited states in ^{13}N were studied through the $(^3\text{He}, t)$ and $(^3\text{He}, tp)$ reactions. The measurements of the $(^3\text{He}, t)$, $(^3\text{He}, tp)$, and $(^3\text{He}, ^3\text{He})$ reactions on ^{13}C were performed at the bombarding energy of 150 MeV/nucleon. To obtain the phenomenological optical-potential parameters, elastic scattering of ^3He particles from ^{13}C was measured at the scattering angles of $\theta_{\text{lab}} = 2^\circ - 22^\circ$. The angular distributions of cross sections for the $^{13}\text{C}(^3\text{He}, t)^{13}\text{N}$ reaction were obtained at $\theta_{\text{lab}} = 0^\circ - 17^\circ$. Decayed protons from the excited states in ^{13}N were measured in coincidence with tritons from the $(^3\text{He}, t)$ reactions at the scattering angle of 0° .

Microscopic DWBA calculations of the $^{13}\text{C}(^3\text{He}, t)^{13}\text{N}$ reactions were performed at 150 MeV/nucleon with the program code DWBA98 and compared to the experimental results. The effective interaction used had the same form as obtained at lower incident energies, but the strengths of each term were modified to fit the obtained angular distributions. Several transition densities in both the $0\hbar\omega$ and $2\hbar\omega$ spaces were used. There were slight differences between the calculated results with different transition densities. The shapes of the experimental differential cross sections for GT states were reasonably reproduced in the calculations.

The branching ratios for decay from the GT states in ^{13}N to the low-lying ^{12}C $T=0$ state were determined. The experi-

mental branching ratios disagreed with the prediction of shell-model calculations. At the present stage, there is no two-body interaction which consistently reproduces the branching ratios of all the GT states. The branching ratios give a severe limitation on the nuclear wave function. It is demonstrated that the proton-decay data can be a good means to test the microscopic structure of nuclear wave functions.

Recently, Tohsaki *et al.* reported that the 0_2^+ state in ^{12}C is a dilute Bose condensed state of three α particles [8]. The dilute states have a reduced density and it was found that the wave function of the 7.65-MeV 0_2^+ state in ^{12}C expands spatially very much compared with that of the ground state (0_1^+). Under this assumption, the spin-orbit splitting felt by an extra nucleon is correspondingly weakened. The spin-orbit pair of the $1/2^-$ and $3/2^-$ orbitals with respect to the $^{12}\text{C}(0_2^+)$ state correspond to the 8.92-MeV $1/2^-$ and 9.48-MeV $3/2^-$ states in ^{13}N [11], respectively. These two states can not decay to the 7.65-MeV 0_2^+ in ^{12}C , energetically. Around 10 MeV in ^{12}C , there is the 0_3^+ state with a width of around 3 MeV. This state is also expected to have 3α cluster structure. The spin-orbit partners coupled with the 0_3^+ state could be the 10.83-MeV $1/2^-$ and 11.88-MeV $3/2^-$ states. We can recognize from Table III that the pair with $^{12}\text{C}(0_3^+) + p$ configuration prefer to decay to the 7.65-MeV 0_2^+ in ^{12}C even it can be energetically allowed to decay to the ground 0_1^+ state. This supports the existence of the dilute Bose condensed state with a 3α -cluster configuration. To reproduce the experimental branching ratios of proton decay, we may need to take into account the 3α -cluster wave functions for a more detailed comparison.

ACKNOWLEDGMENTS

The authors are indebted to Professor Otsuka and Professor Suzuki for performing shell-model calculations by using their two-body interactions. They thank Professor Yamada and Professor Horiuchi for many valuable discussions about the α cluster states in ^{12}C . We acknowledge the RCNP cyclotron staff for their support during the course of the present experiment. The present work is supported in part by the Japan Society for the Promotion of Science (JSPS).

-
- [1] R. E. Marrs, E. G. Adelberger, K. A. Snover, and M. D. Cooper, Phys. Rev. Lett. **35**, 202 (1975).
 - [2] E. G. Adelberger, R. E. Marrs, and K. A. Snover, Phys. Rev. C **19**, 1 (1979).
 - [3] S. S. Hanna, Nucl. Phys. **A577**, 173 (1994).
 - [4] S. Suzuki, T. Saito, K. Takahisa, C. Takakuwa, T. Nakagawa, T. Tohei, and K. Abe, Phys. Rev. C **60**, 034309 (1999).
 - [5] H. Akimune, I. Daito, Y. Fujita, M. Fujiwara, M. B. Greenfield, M. N. Harakeh, T. Inomata, J. Jänecke, K. Katori, S. Nakayama, H. Sakai, Y. Sakemi, M. Tanaka, and M. Yosoi, Phys. Lett. B **323**, 107 (1994).
 - [6] H. Akimune, I. Daito, Y. Fujita, M. Fujiwara, M. B. Greenfield, M. N. Harakeh, T. Inomata, J. Jänecke, K. Katori, S. Nakayama, H. Sakai, Y. Sakemi, M. Tanaka, and M. Yosoi, Phys. Rev. C **52**, 604 (1995).
 - [7] K. Hara, K. T. Adachi, H. Akimune, I. Daito, H. Fujimura, Y. Fujita, M. Fujiwara, K. Fushimi, K. Y. Hara, M. N. Harakeh, K. Ichihara, T. Ishikawa, J. Jänecke, J. Kamiya, T. Kawabata, K. Kawase, K. Nakanishi, Y. Sakemi, Y. Shimbara, Y. Shimizu, M. Uchida, H. P. Yoshida, M. Yosoi, and R. G. T. Zegers, Phys. Rev. C **68**, 064612 (2003).
 - [8] A. Tohsaki, H. Horiuchi, P. Schuck, and G. Röpke, Phys. Rev.

- Lett. **87**, 192501 (2001).
- [9] Y. Funaki, A. Tohsaki, H. Horiuchi, P. Schuck, and G. Röpke, Phys. Rev. C **67**, 051306 (2003).
 - [10] T. Yamada and P. Schuck, Phys. Rev. C **69**, 024309 (2004).
 - [11] T. Yamada, H. Horiuchi, and P. Schuck (private communication); P. Schuck (unpublished).
 - [12] M. Fujiwara, H. Akimune, I. Daito, H. Fujimura, Y. Fujita, K. Hatanaka, H. Ikegami, I. Katayama, K. Nagayama, N. Matsuoka, S. Morinobu, T. Noro, M. Yoshimura, H. Sakaguchi, Y. Sakemi, A. Tamii, and M. Yosoi, Nucl. Instrum. Methods Phys. Res. A **422**, 484 (1999).
 - [13] H. Akimune, I. Daito, H. Fujimura, M. Fujiwara, T. Inomata, A. Tamii, H. Toyokawa, and M. Yosoi, RCNP annual report, 1996 (unpublished), p. 119.
 - [14] F. Ajzenberg-Selove, Nucl. Phys. **A360**, 1 (1981); **A449**, 1 (1986); **A523**, 1 (1991).
 - [15] X. Yang, L. Wang, J. Rapaport, C. D. Goodman, C. C. Foster, Y. Wang, E. Sugarbaker, D. Marchlinski, S. de Lucia, B. Luther, L. Rybaryk, T. N. Taddeucci, and B. K. Park, Phys. Rev. C **52**, 2535 (1995).
 - [16] A. Erell, J. Alster, J. Lichtenstadt, A. Moinester, J. D. Bowman, M. D. Cooper, F. Irom, H. S. Matis, E. Piasetzky, and U. Sennhauser, Phys. Rev. C **34**, 1822 (1986).
 - [17] L. Wang, X. Yang, J. Rapaport, C. D. Goodman, C. C. Foster, Y. Wang, J. Piekarewicz, E. Sugarbaker, D. March, S. de Lucia, B. Luther, L. Rybaryk, T. N. Taddeucci, and B. K. Park, Phys. Rev. C **50**, 2438 (1994).
 - [18] J. Raynal, computer code DWBA98, NEA 1209/05, 1999.
 - [19] B. A. Brown *et al.* The Oxford-Buenos Aires-MSU shell model code, OXBASH, Michigan State University Cyclotron Laboratory, Report No. 524, 1986.
 - [20] S. Cohen and D. Kurath, Nucl. Phys. **73**, 1 (1965).
 - [21] E. K. Warburton and B. A. Brown, Phys. Rev. C **46**, 923 (1992).
 - [22] D. J. Millener and D. Kurath, Nucl. Phys. **A255**, 315 (1975).
 - [23] T. Otsuka, R. Fujimoto, Y. Utsuno, B. A. Brown, M. Honma, and T. Mizusaki, Phys. Rev. Lett. **87**, 082502 (2001).
 - [24] T. Suzuki (private communication).
 - [25] J. Raynal, Coupled-channel computer-code ECIS79, CEA Report No. CEA-N-2772 1994.
 - [26] S. Y. van der Werf, S. Brandenburg, P. Gradijk, W. A. Sterrenburg, M. N. Harakeh, M. B. Greenfield, B. A. Brown, and M. Fujiwara, Nucl. Phys. **A469**, 305 (1989).
 - [27] R. G. T. Zegers, A. M. van den Berg, S. Brandenburg, M. Fujiwara, J. Guillot, M. N. Harakeh, H. Laurent, S. Y. van der Werf, A. Willis, and H. W. Wilschut, Phys. Rev. C **63**, 034613 (2001).
 - [28] R. G. T. Zegers, H. Abend, H. Akimune, A. M. van den Berg, H. Fujimura, H. Fujita, Y. Fujita, M. Fujiwara, S. Gales, K. Hara, M. N. Harakeh, T. Ishikawa, T. Kawabata, K. Kawase, T. Mibe, K. Nakanishi, S. Nakayama, H. Toyokawa, M. Uchida, T. Yamagata, K. Yamasaki, and M. Yosoi, Phys. Rev. Lett. **90**, 202501 (2003).
 - [29] R. Schaeffer, Nucl. Phys. **A164**, 145 (1971).
 - [30] H. Akimune, H. Ejiri, M. Fujiwara, I. Daito, T. Inomata, R. Hazama, A. Tamii, H. Toyokawa, and M. Yosoi, Phys. Lett. B **394**, 23 (1997).
 - [31] I. Daito, H. Akimune, Sam M. Austin, D. Bazin, G. P. A. Berg, J. A. Brown, B. S. Davids, Y. Fujita, H. Fujimura, M. Fujiwara, R. Hazama, T. Inomata, K. Ishibashi, J. Jänecke, S. Nakayama, K. Pham, D. A. Roberts, B. M. Sherill, M. Steiner, A. Tamii, M. Tanaka, H. Toyokawa, and M. Yosoi, Phys. Lett. B **418**, 27 (1998).
 - [32] X. Wang, J. Rapaport, M. Palarczyk, C. Hautala, X. Yang, D. L. Prout, I. Van Heerden, R. Howes, S. Parks, E. Sugarbaker, and B. A. Brown, Phys. Rev. C **63**, 024608 (2001).
 - [33] X. Wang, J. Rapaport, M. Palarczyk, C. Hautala, X. Yang, D. L. Prout, B. Anderson, A. R. Baldwin, J. Olmsted, J. W. Watson, W.-M. Zhang, I. Van Heerden, E. J. Stephenson, R. Howes, S. Parks, E. Sugarbaker, B. A. Brown, and F. Sammaruca, Phys. Rev. C **66**, 014606 (2002).
 - [34] F. G. Perey, Phys. Rev. **131**, 745 (1963); C. M. Perey and F. G. Perey, At. Data Nucl. Data Tables **17**, 1 (1974).